



Figures and figure supplements

Sensing of nutrients by CPT1C regulates late endosome/lysosome anterograde transport and axon growth

Marta Palomo-Guerrero *et al*

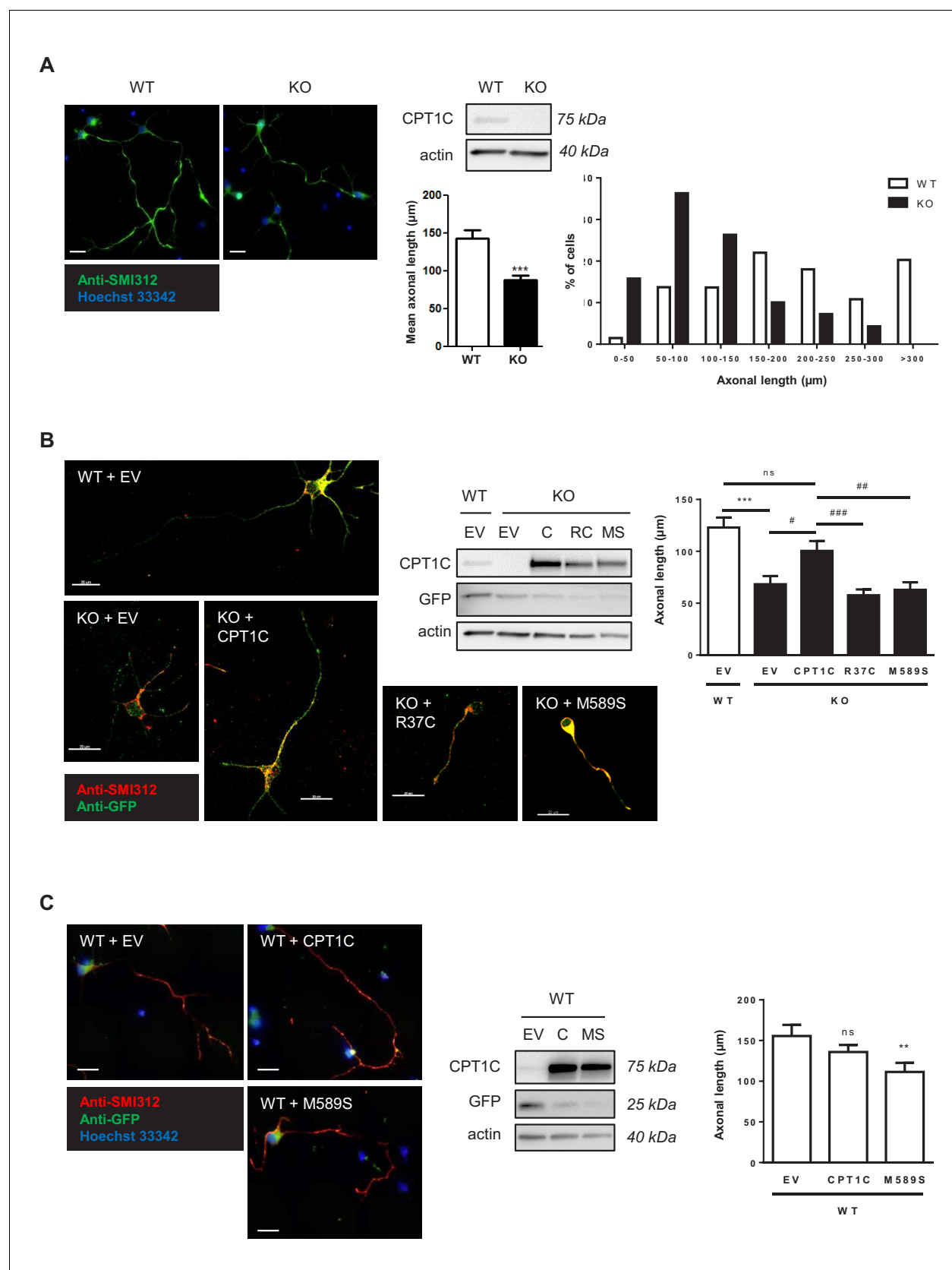


Figure 1. CPT1C is necessary for proper axon growth. (A) Primary cortical neurons derived from WT and *Cpt1c* KO E16 mouse embryos were cultured and fixed at 4DIV. Then, axons were labeled with a specific marker (SMI-312; in green) and nuclei were detected with Hoechst staining (blue). CPT1C

Figure 1 continued on next page

Figure 1 continued

absence in KO cultures was corroborated by western blot. Axonal length was analyzed from three independent experiments performed in biological triplicates. Right graph shows the percentage of cells with axons of a certain length (intervals of 50 μm), while in left graph the mean \pm SEM of all axons is shown ($n = 100$ cells per genotype; Student's t test; *** $p < 0.001$). (B) *Cpt1c* KO neurons were infected at 1DIV with lentiviral vectors that codified for mouse CPT1C or the mutated forms M589S (MS) or R37C (RC). At 4DIV, cells were fixed and axon was identified as described above. GFP was used to detect infected cells. Immunoblotting was performed to confirm CPT1C and M589S expression in infected KO neurons. Graph shows the mean axonal length \pm SEM of 2 independent experiments performed in biological duplicates ($n = 50$ cells per condition; One-way ANOVA followed by Bonferroni's comparison test; *** $p < 0.001$ versus WT + EV and # $p < 0.05$, ## $p < 0.01$ and ### $p < 0.001$ versus KO + CPT1C). (C) Effect of M589S overexpression in WT cells. Graph shows the mean axonal length \pm SEM of 2 independent experiments performed in biological duplicates ($n = 50$ cells per condition; One-way ANOVA followed by Bonferroni's comparison test; ** $p < 0.01$ versus WT + EV). Scale bar, 20 μm .

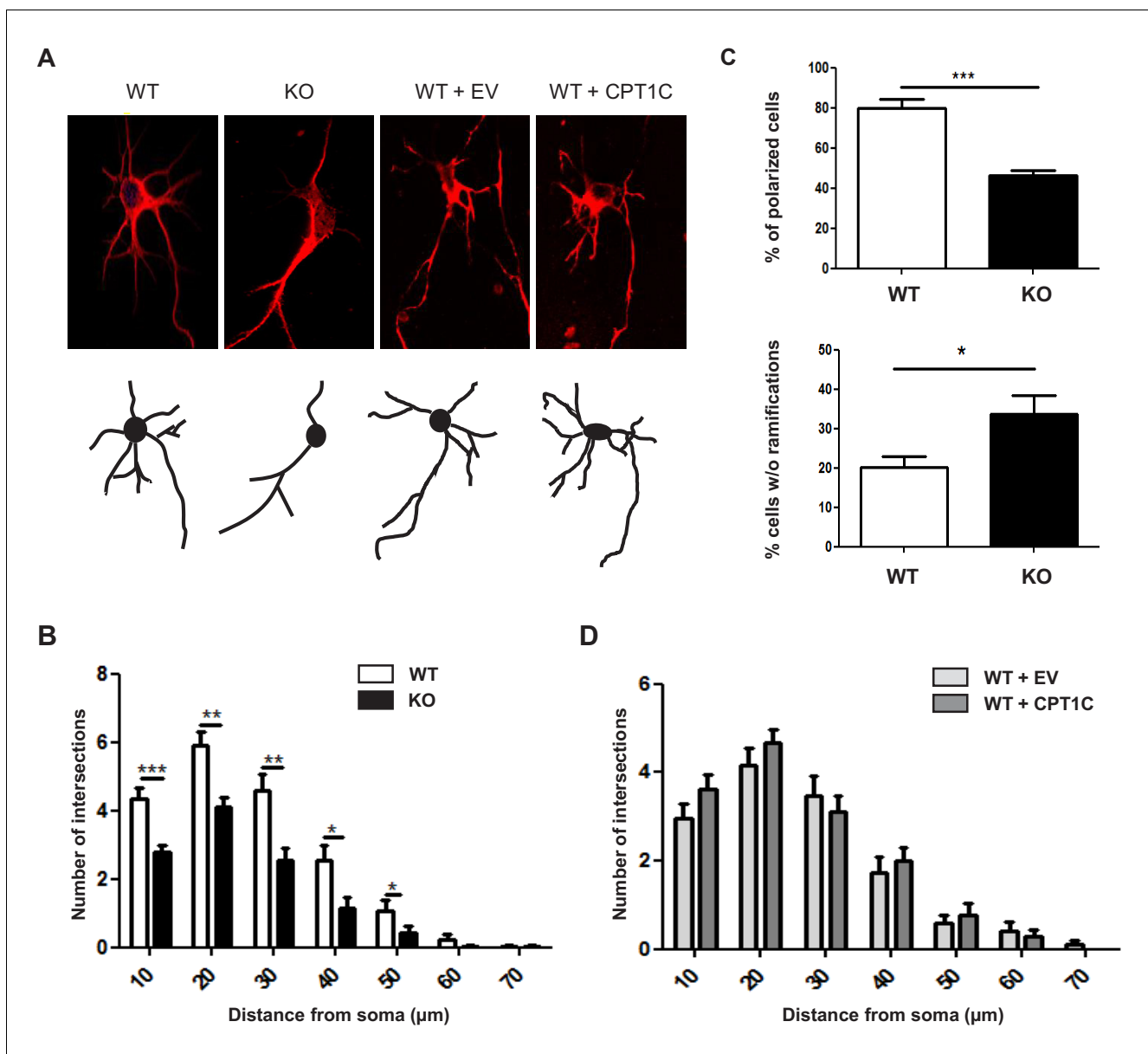


Figure 1—figure supplement 1. Dendritic arborization of *Cpt1c* KO cortical neurons. WT or *Cpt1c* KO neurons were seeded and infected as explained in **Figure 1**. Dendritic arborization was analyzed using the Sholl method. **(A)** Representative images are shown. **(B)** Number of dendritic intersections with concentric circles of different radius (distance to soma) in WT and KO neurons. Results are the mean \pm SEM of 3 independent experiments performed in biological triplicates ($n = 100$ cells per genotype; Two-way ANOVA followed by Bonferroni's comparison test; $*p < 0.05$, $**p < 0.01$ and $***p < 0.001$). **(C)** Percentage of polarized cells (above) and percentage of cells without ramifications (below). Values are the mean \pm SEM of 3 independent experiments performed in biological triplicates ($n = 100$ cells per genotype; Student's t test; $*p < 0.05$ and $***p < 0.001$). **(D)** Number of dendritic intersections with concentric circles of different radius (distance to soma) in CPT1C-overexpressing neurons. Values are the mean \pm SEM of 3 independent experiments performed in biological triplicates ($n = 100$ cells per condition; Two-way ANOVA followed by Bonferroni's comparison test; $p > 0.05$). Scale bar, $10 \mu\text{m}$.

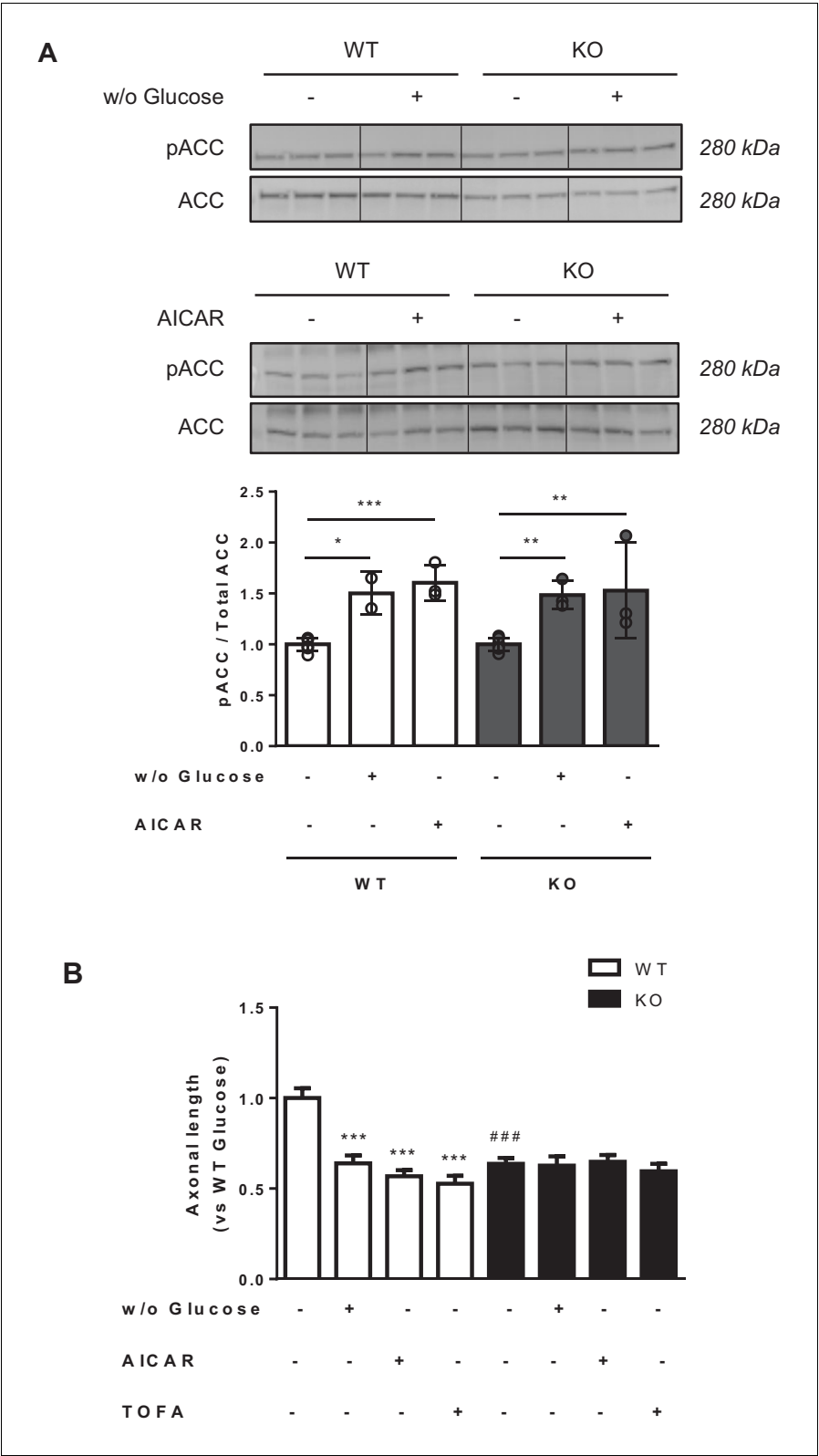


Figure 2. Metabolic stress decreases axon growth through CPT1C. 3DIV primary cortical neurons derived from WT and KO CPT1C embryos were incubated with DMEM medium with (25 mM) or without glucose (2 hr), treated with AICAR (1.5 hr at 2.5 mM), TOFA (1.5 hr at 20 μ g/mL) or vehicle (DMSO 1:500). At the end of the treatment, the medium was replaced by Neurobasal + B27 conditioned medium. 24 hr later (at 4DIV), cells were fixed and

Figure 2 continued on next page

Figure 2 continued

processed by immunostaining with anti-SMI-312. (A) ACC phosphorylation (inhibition) by glucose depletion or AICAR treatment in WT and *Cpt1c* KO neurons was corroborated by Western blot. For quantification, the ratio between pACC and total ACC levels was used. Results are the mean \pm SD of biological triplicates ($n = 3$ samples per condition; Two-way ANOVA followed by Bonferroni's multiple comparison test; * $p < 0.05$, ** $p < 0.01$ and *** $p < 0.001$ versus control treatment within the same genotype). (B) Mean axon length quantification. The neurofilament marker SMI-312R was used as axon marker. Results are shown as the mean \pm SEM of 3 independent experiment performed in biological duplicates ($n = 35$ – 60 cells per condition; Two-way ANOVA followed by Bonferroni's multiple comparison test; *** $p < 0.001$ versus control treatment and #### $p < 0.001$ versus WT within the same treatment).

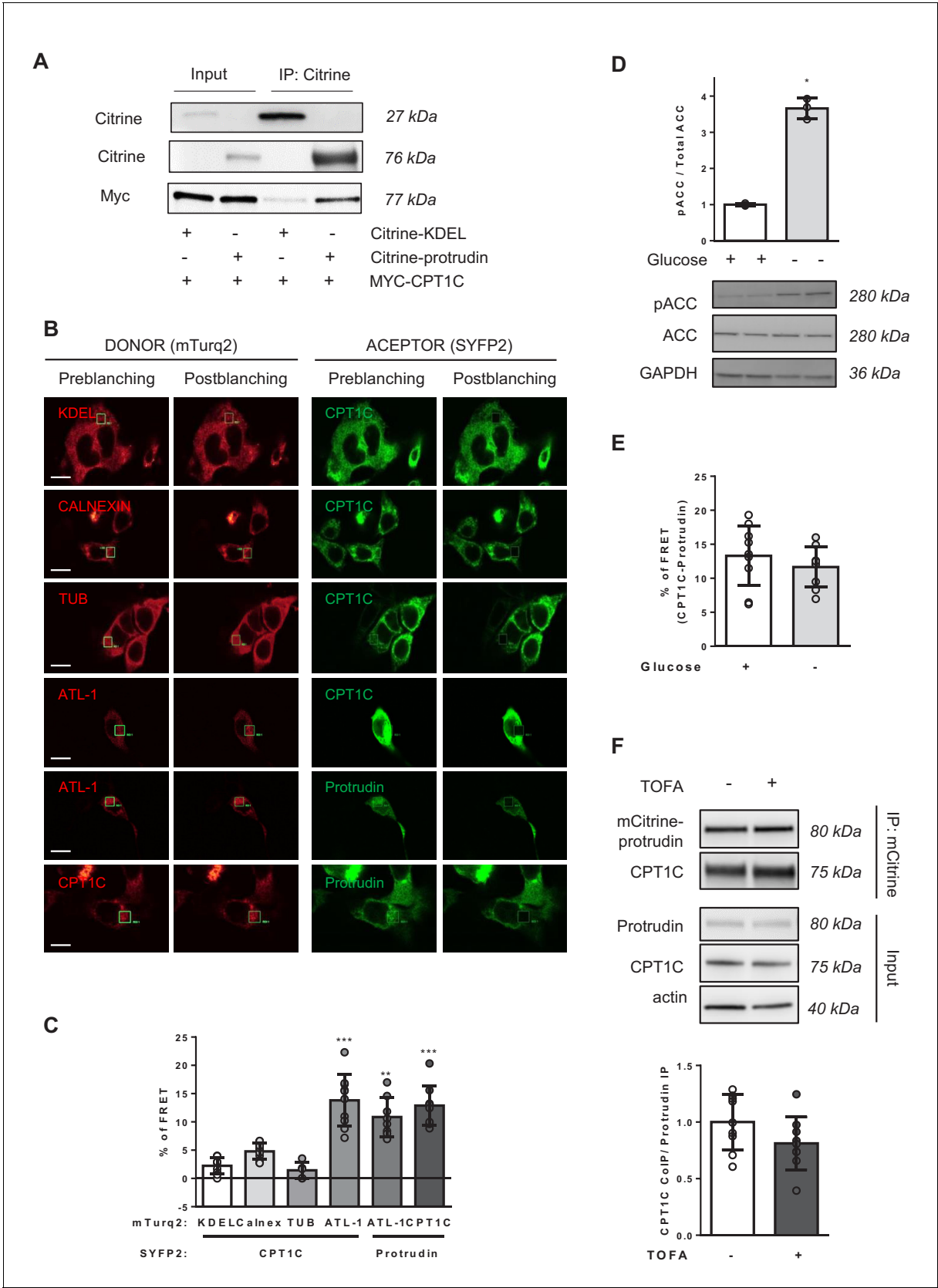


Figure 3 continued

with the GFP-Trap assay, and the indicated proteins were detected by immunoblot in whole lysate (input) and immunoprecipitated samples (IP). The co-IP was performed in biological triplicates. A representative image of the experiment is shown. **(B–C)** Binding evaluation by FRET assay in HEK293 cells. Percentage of FRET was measured by the increase of donor intensity after photobleaching. mTurquoise-ER (KDEL), mTurquoise-calnexin and Tubulin-mTurquoise2 (TUB) with CPT1C-SYFP2 were used as negative interactions, while Atlantin1-mTurquoise2 (ATL1) with protrudin-SYFP2 and atlastin-1-mTurquoise2 with CPT1C-SYFP2, as positive controls. Representative images of transfected cells with proteins fused to mTurquoise2 (donor; red) or SYFP2 (acceptor; green) are shown in B. Scale bar, 20 μ m. Values are shown in C as mean \pm SD of 2 independent experiments performed in biological duplicates (n = 5–11 cells per condition were analyzed; One-way ANOVA followed by Bonferroni's multiple comparison test; **p<0.001 and ***p<0.001 vs KDEL control). **(D)** ACC phosphorylation after 4 hr of glucose deprivation in HEK293 cells was confirmed by Western blot. Graph shows the mean \pm SD of biological triplicates (n = 3 samples per condition; Mann-Whitney U test; *p=0.05). **(E–F)** CPT1C-protrudin interactions under metabolic stress conditions. In E, HEK293 cells were incubated in complete medium (25 mM of glucose) or with a medium without glucose (4 hr) and CPT1C-protrudin interaction was analyzed by FRET assay. Results are given as mean \pm SD of 2 independent experiments performed in biological duplicates (n = 9–10 cells per condition; Student's t test; p=0.4315). In F, CPT1C stably expressing HeLa cells, were transfected with mCitrine-protrudin for 24 hr and treated with TOFA (1 hr at 20 μ g/mL). Immunoprecipitation was used to analyze CPT1C-protrudin binding. Results are given as mean \pm SD of 2 independent experiments performed in biological quadruplicates or quintuplicates (n = 9 samples per condition; Student's t test; p=0.1142).

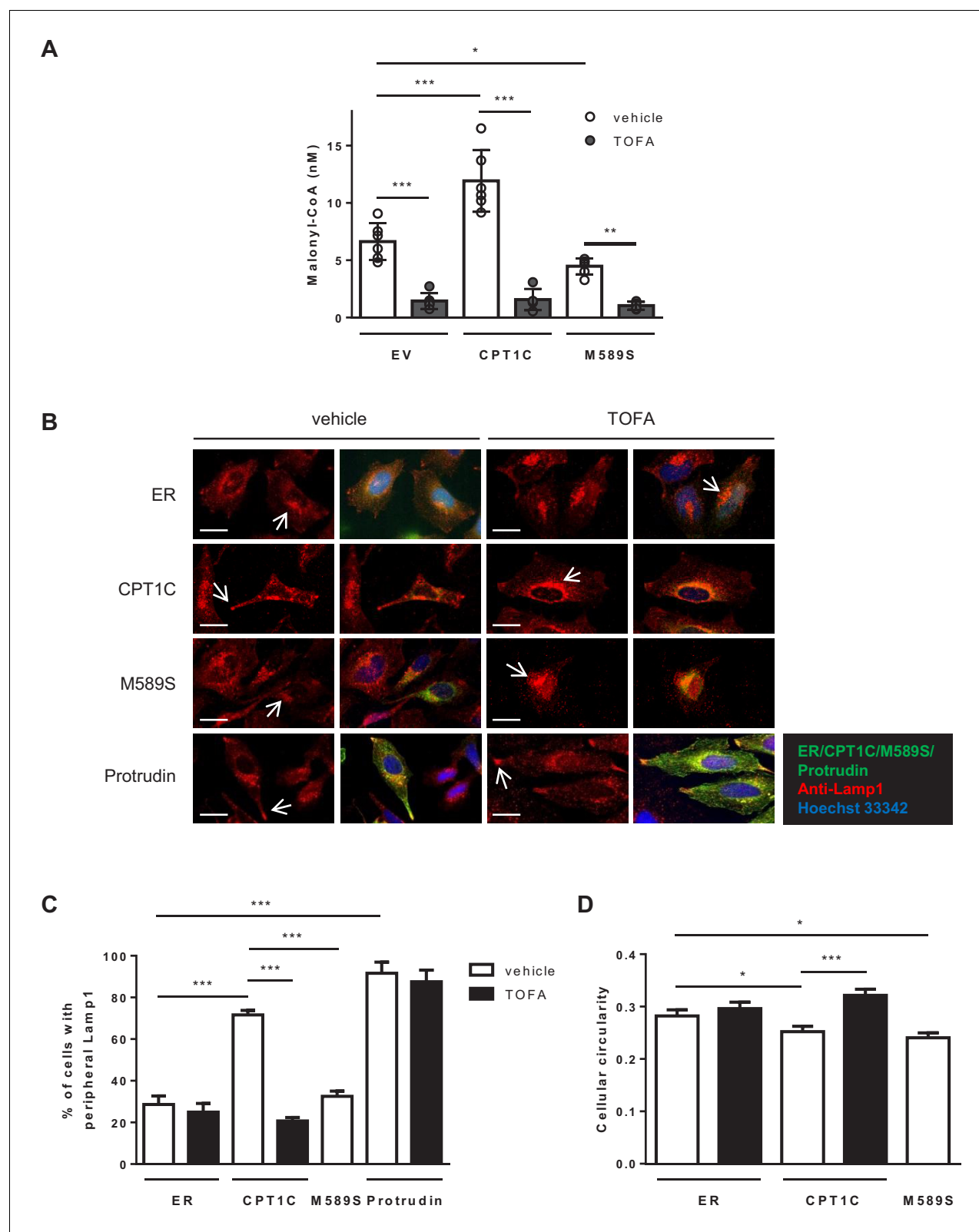


Figure 4. CPT1C overexpression promotes the peripheral localization of Lamp1-positive vesicles depending on malonyl-CoA levels. (A) Intracellular malonyl-CoA levels decrease after TOFA treatment. HeLa cells stably expressing empty vector, CPT1C or CPT1C^{M589S} were treated with TOFA (1 hr at 20 μ g/mL) or the vehicle (DMSO; 1:500). Then, cells were collected and processed as explained in Materials and methods section for malonyl-CoA levels determination. Raw data are the mean of technical duplicates. Results are the mean \pm SD of 2 independent experiments performed in biological replicates. (B) Fluorescence microscopy images of HeLa cells expressing EV, CPT1C, M589S or Protrudin, treated with vehicle or TOFA. Staining: ER/CPT1C/M589S/Protrudin (green), Anti-Lamp1 (red), Hoechst 33342 (blue). White arrows indicate peripheral localization of Lamp1-positive vesicles. (C) Bar graph showing the percentage of cells with peripheral Lamp1 staining for EV, CPT1C, M589S and Protrudin under vehicle (white bars) and TOFA (black bars) treatment. TOFA treatment significantly reduces the percentage of cells with peripheral Lamp1 staining in all conditions. (D) Bar graph showing cellular circularity for EV, CPT1C and M589S cells treated with vehicle (white bars) or TOFA (black bars). TOFA treatment increases cellular circularity in EV and CPT1C cells.

Figure 4 continued

triplicates ($n = 4\text{--}6$ total samples; Two-way ANOVA followed by Bonferroni's multiple comparison test; $*p < 0.05$, $**p < 0.01$ and $***p < 0.001$). (B) Representative images of HeLa cells transfected with CPT1C-mTurquoise2, CPT1C^{M589S}-mTurquoise2 or mTurquoise-ER (shown in green) and immunostained with anti-Lamp1 (in red). Scale bar, 20 μm . White arrows show the accumulation of Lamp1-positive vesicles. (C) Percentages of cells with peripheral localization of Lamp1. (D) Quantification of cellular circularity. Values in C and D are shown as mean \pm SEM of 5 independent experiments performed in biological duplicates ($n = 100$ cells per condition were analyzed; One-way ANOVA, followed by Bonferroni's comparison test; $*p < 0.05$ and $***p < 0.001$).

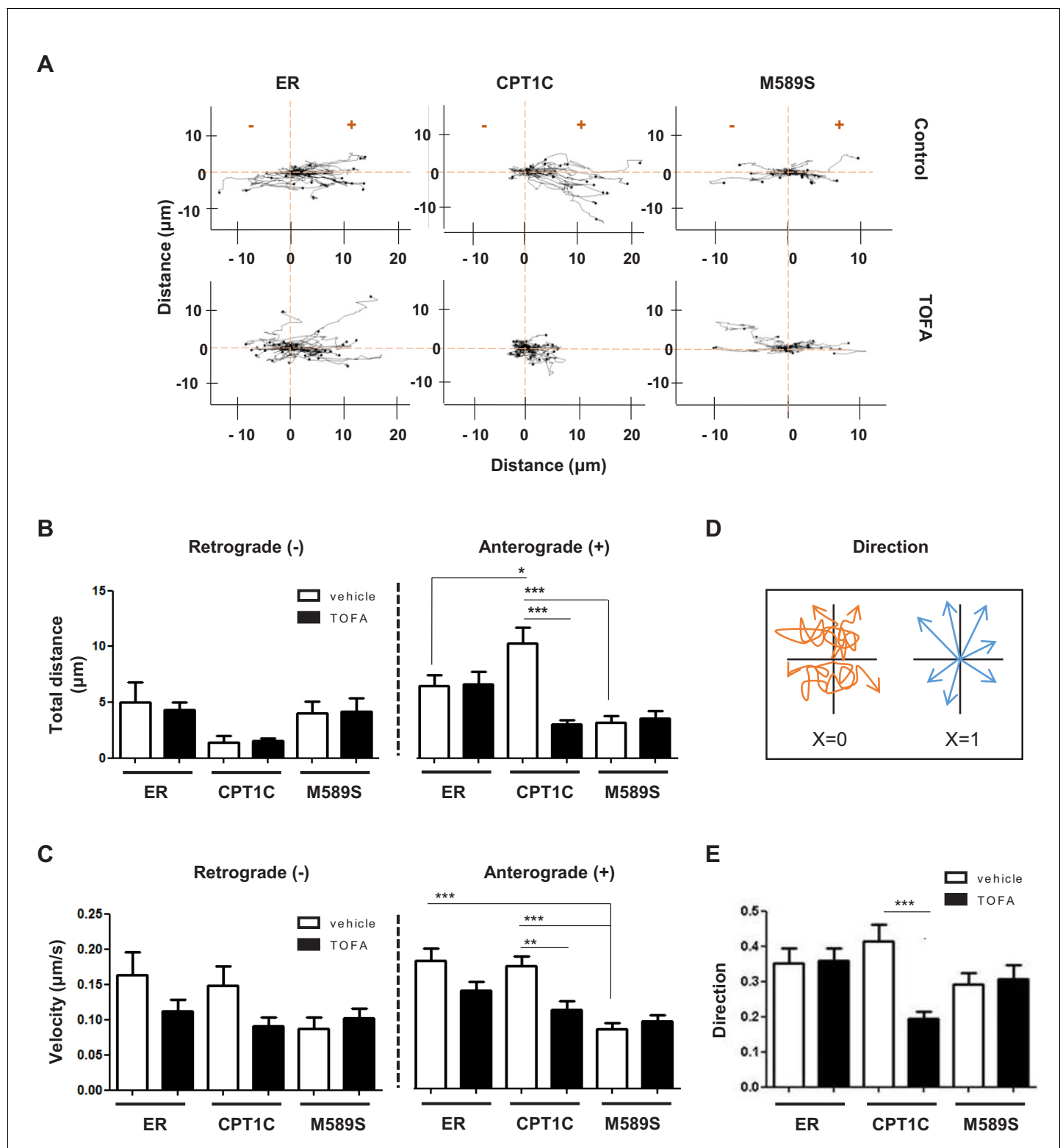


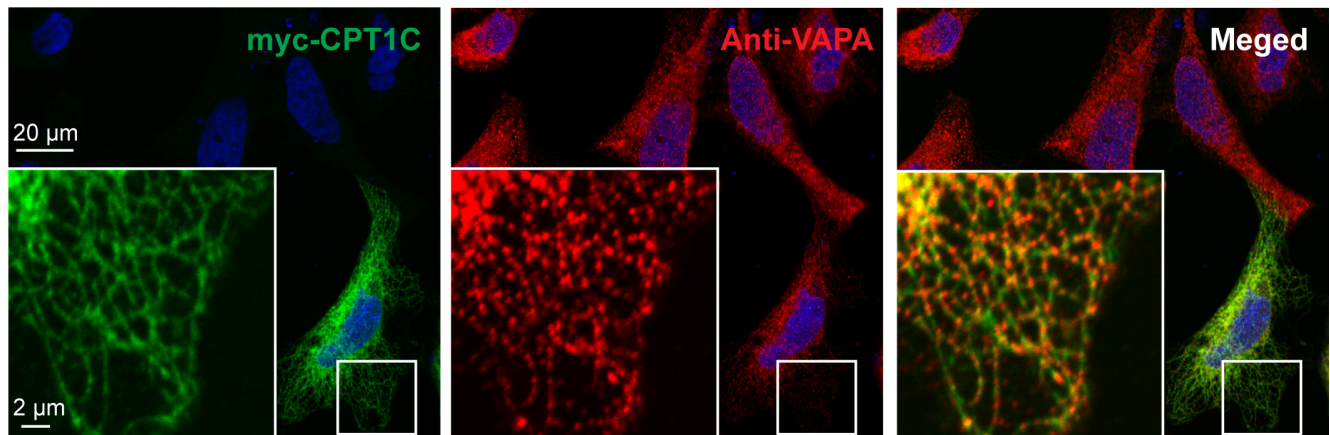
Figure 5. CPT1C regulates the anterograde transport of LEs depending on malonyl-CoA levels. HeLa cells were co-transfected with mTurquoise-ER, CPT1C-mTurquoise2 or CPT1C^{M589S}-mTurquoise2, and mCherry-FYCO1. After 48 hr, cells were treated with TOFA (1 hr at 20 $\mu\text{g}/\text{mL}$) or vehicle (control, DMSO 1:500) for 1 hr. Trajectories of mCherry-FYCO1 vesicles were analyzed. Representative videos are shown in **Figure 5—videos 1–6**. (A) Movement pattern of individual mCherry-FYCO1 vesicles in two dimensions. (B) Total distance traveled in anterograde and retrograde directions. (C) Quantification of vesicle velocity. (D) Scheme for the direction quantification. The random movement of the vesicles was considered value 0, and the

Figure 5 continued on next page

Figure 5 continued

directional movement value 1. (E) Analysis of vesicle directionality. Results are shown as mean \pm SEM of 3 independent experiments performed in biological duplicates (n = 30–40 vesicles per condition were analyzed; Two-way ANOVA followed by Bonferroni's comparison test; *p<0.05, **p<0.01 and ***p<0.001).

A



B

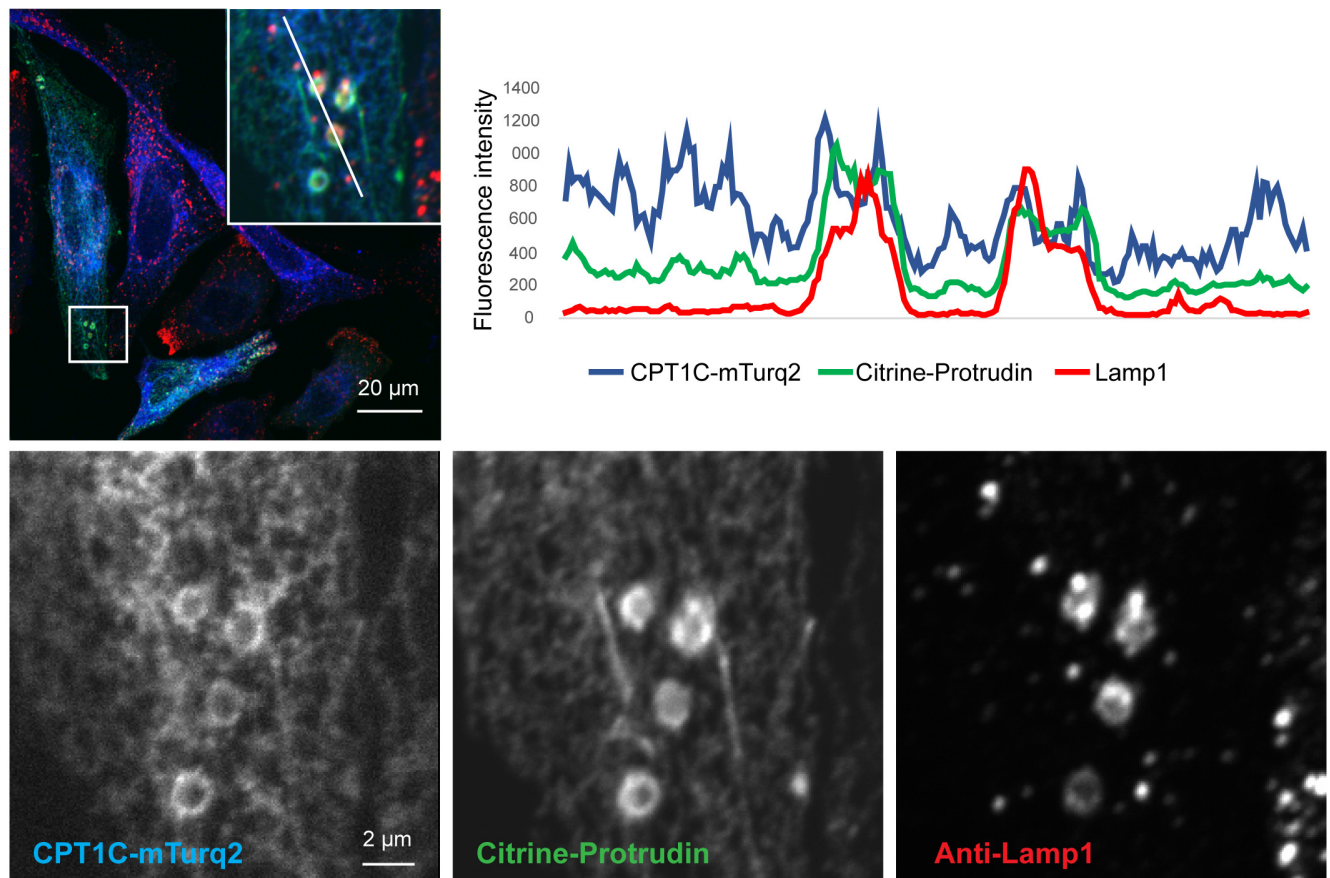


Figure 6. CPT1C is an ER protein localizing to ER-LE/Ly contact sites. HeLa cells were transfected with the plasmids indicated, fixed in 3% FA, stained with the indicated antibodies and analyzed by confocal microscopy. **(A)** Myc-CPT1C colocalizes with the ER resident protein VAPA. **(B)** CPT1C-mTurq2 colocalizes with the ER protein protrudin in ER-LE/Ly contact sites, but is not enriched in contact sites, contrary to protrudin (intensity line plot).

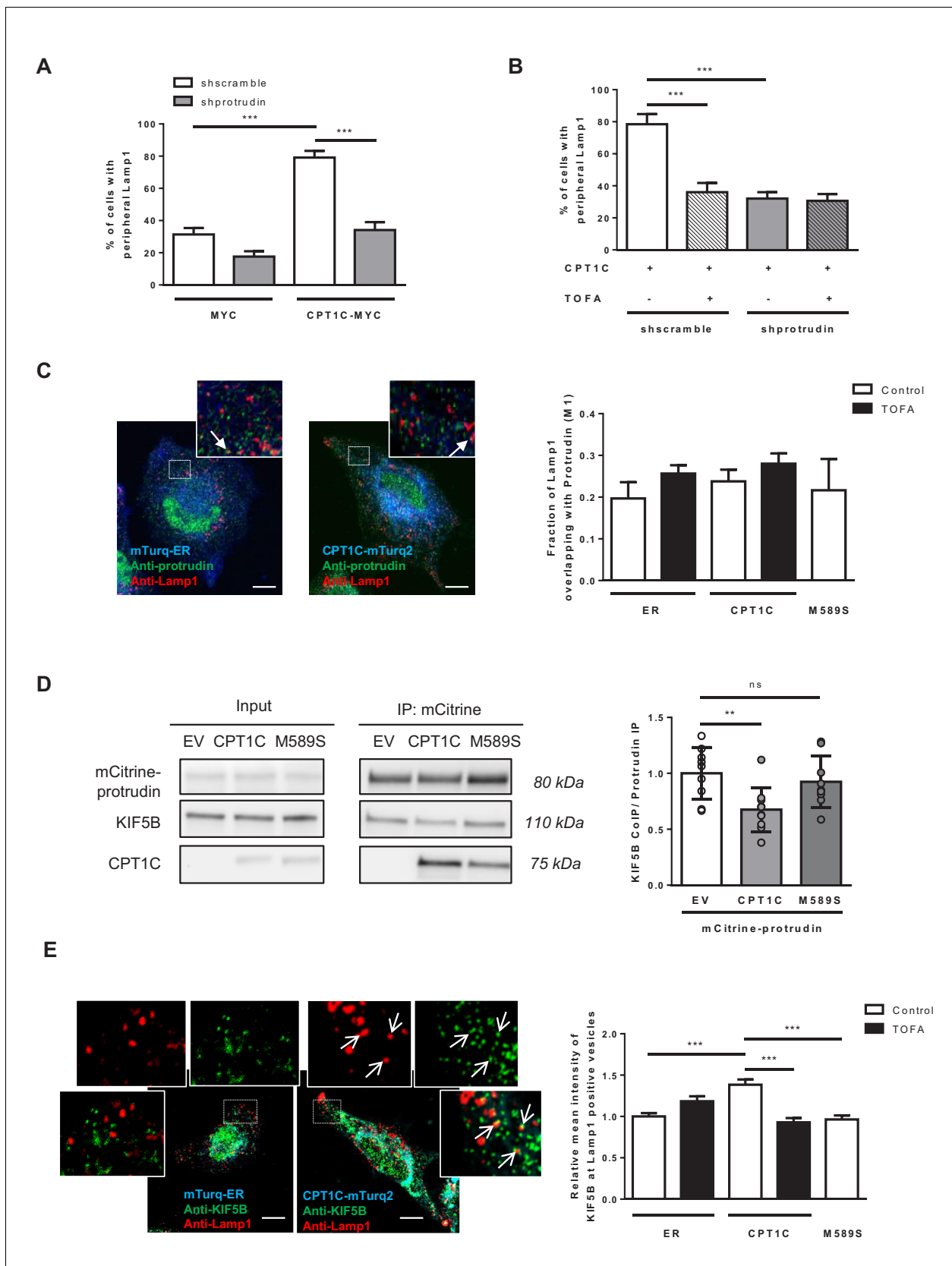


Figure 7. CPT1C regulates the protrudin-mediated transfer of kinesin-1 to LE/Lys in a malonyl-CoA-dependent manner. (A) Plasmids for protrudin silencing and CPT1C overexpression were transfected in HeLa cells at the same time. A scrambled sequence was used as a negative control of Figure 7 continued on next page

Figure 7 continued

protrudin silencing, and an empty vector (Myc) was used as negative control of CPT1C overexpression. 72 hr later, Lamp1 localization was analysed by immunostaining. Results are shown as the percentage of cells with peripheral Lamp1 and given as mean \pm SEM of 3 independent experiments performed in biological duplicates (n = 100 cells per condition were analyzed; Two-way ANOVA followed by Bonferroni's comparison test; ***p<0.001). (B) Percentage of cells with peripheral Lamp1 under TOFA treatment. Cells processed as in A were treated with TOFA (1 hr at 20 μ g/mL) or vehicle (control, DMSO 1:500). Values are the mean \pm SEM of 2 independent experiments performed in biological duplicates (n = 100 cells per condition were analyzed; Two-way ANOVA followed by Bonferroni's comparison test; ***p<0.001). (C) Fraction of Lamp1 overlapping with protrudin. Cells were transfected with mTurquoise-ER, CPT1C-mTurquoise2 or CPT1C^{M589S}-mTurquoise2 and 48 hr later treated with TOFA for 1 hr. Then, a double immunostaining was achieved to detect protrudin and Lamp1 by confocal microscopy. Representative images (left) and quantification results (right) are shown. Results are given as Manders overlap coefficient M_1 (the fraction of Lamp1 in compartments containing protrudin). Values are the mean \pm SEM of 3 independent experiments performed in biological duplicates (n = 30 cells per condition; One-way ANOVA followed by Bonferroni's comparison test; p>0.05). (D) KIF5B recruitment by protrudin. EV, CPT1C or M589S stably expressing cells were transfected with mCitrine-protrudin. 24 hr later, mCitrine-protrudin was immunoprecipitated. The expression of protrudin, KIF5B and CPT1C was evaluated by Western blot in whole lysates (input) and immunoprecipitated samples (IP). Results are given as the mean \pm SD of 3 independent experiments performed in biological duplicates, triplicates or quadruplicates (n = 9–10 samples per condition; One-way ANOVA followed by Bonferroni's multiple comparison test; EV vs CPT1C: **p<0.01, and EV vs M589S: p>0.05). (E) Relative mean intensity of KIF5B at Lamp1-positive vesicles. Cells transfected and treated as in C were immunostained with anti-Lamp1 (in red) and anti-KIF5B (in green). Insets show magnification of a part of the region analyzed. Values are the mean \pm SEM of 4 independent experiments performed in biological duplicates (n = 40 cells per condition; One-way ANOVA followed by Bonferroni's comparison test; ***p<0.001). White arrows in C and E show colocalization dots. Scale bar, 10 μ m.

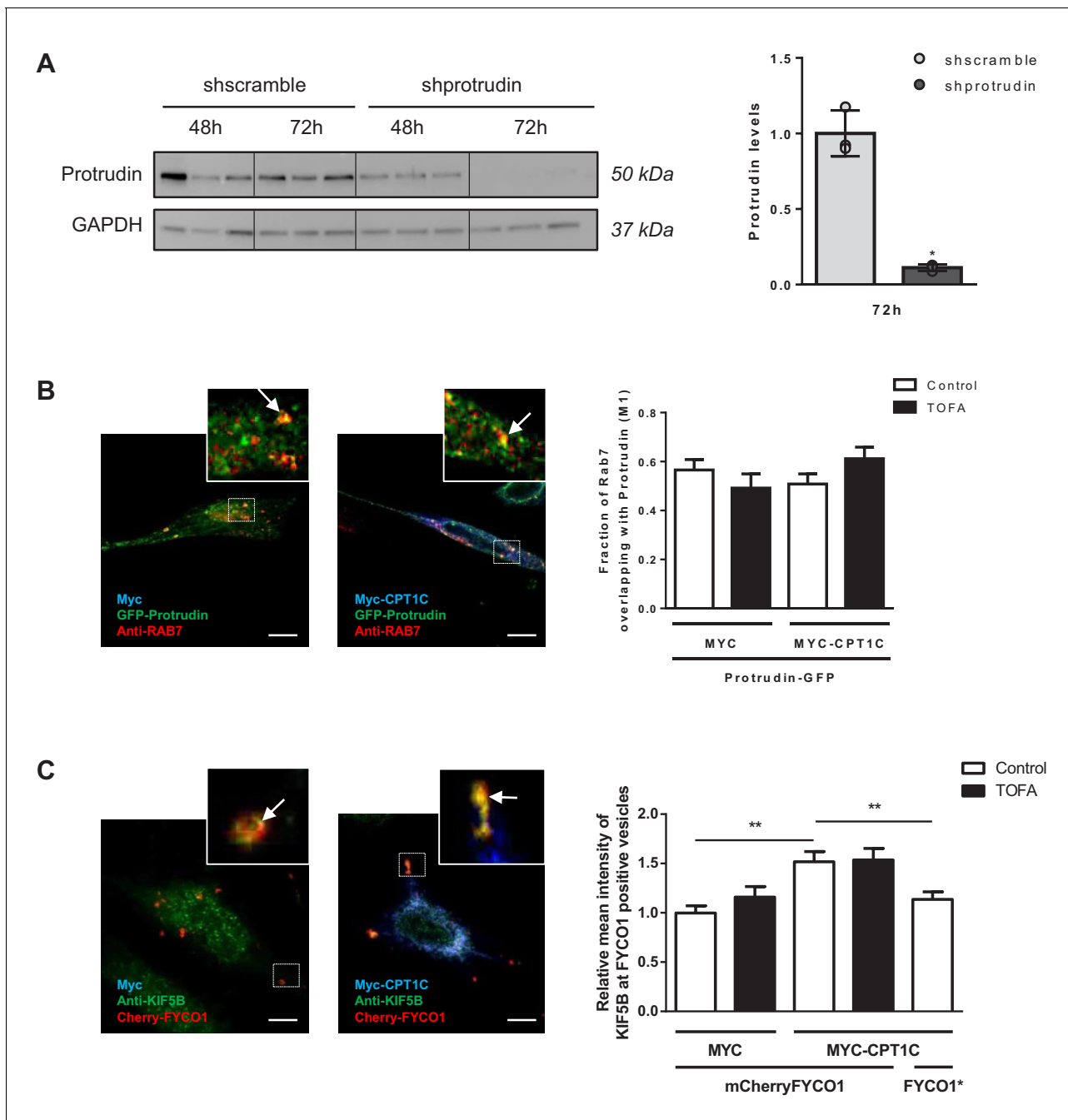


Figure 7—figure supplement 1. CPT1C effects on protrudin-Rab7 colocalization and FYCO1-recruitment of kinesin-1. (A) Protrudin silencing in HeLa cells. Protrudin protein levels were analyzed by Western blot 48 or 72 hr after transfection with shprotrudin or shscramble. GAPDH was used as a loading control. After 72 hr, protrudin silencing was higher than 90%. Values are the mean \pm SD of biological triplicates ($n = 3$ samples per condition; Mann-Whitney U test; * $p=0.05$). (B) Fraction of Rab7 overlapping with protrudin. HeLa cells were transfected with an empty vector (Myc) or Myc-CPT1C and GFP-protrudin and fixed 48 hr later. Rab7 and Myc were labeled with anti-Rab7 and anti-Myc, respectively. Results are given as Manders overlap coefficient M_1 (the fraction of Rab7 in compartments containing protrudin). Results are shown as mean \pm SEM of 2 independent experiments performed in biological duplicates ($n = 30$ cells per condition; Two-way ANOVA followed by Bonferroni's comparison test; $p>0.05$). (C) Relative mean intensity of KIF5B at FYCO1-positive vesicles. MCherry-FYCO1 or mCherry-FYCO1^{A735-773} (FYCO*) were transfected together with Myc-CPT1C or Myc alone. 36 hr later, cells were treated with TOFA for 1 hr and then double immunostaining against Myc and KIF5B. Results are shown as mean \pm SEM of 2 independent experiments performed in biological duplicates ($n = 30$ cells per condition; One-way ANOVA followed by Bonferroni's comparison test; ** $p<0.01$). White arrows show colocalization dots. Scale bar, 10 μ m.

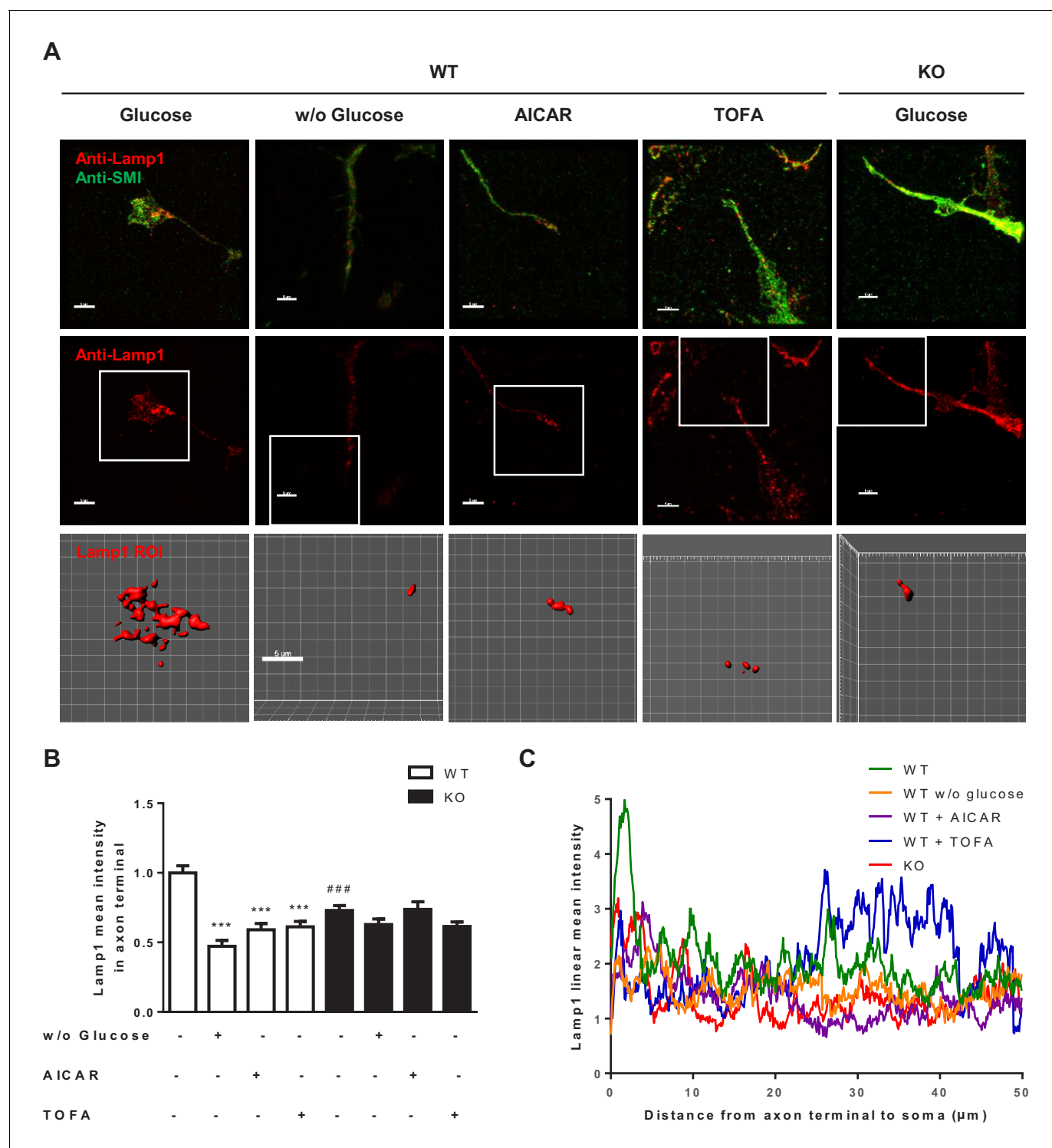


Figure 8. Metabolic stress reduces Lamp1 in axon terminals through CPT1C. 3DIV primary cortical neurons derived from WT and *Cpt1c* KO embryos were treated as in **Figure 2**. 24 hr later (at 4DIV), cells were fixed and processed by immunostaining with anti-Lamp1 and anti-SMI-321 (axon marker). (A) Representative images of the Lamp1 staining at the axon terminal. The region of interest (ROI) selected for the analysis is shown in the amplified square. (B) Lamp1 mean intensity at the axon terminal. The same threshold was used in all the samples. Results are shown as the mean \pm SEM of 3 independent experiment performed in biological duplicates ($n = 35$ – 60 cells per condition; Two-way ANOVA followed by Bonferroni's multiple comparison test; *** $p < 0.001$ versus control treatment and ### $p < 0.001$ versus WT within the same treatment). (C) Lamp1 linear intensity profile. The sum intensity histograms from Z-projection images were analyzed. Due to different axon lengths between groups, only the last $50 \mu\text{m}$ from the axon

Figure 8 continued on next page

Figure 8 continued

terminal to the soma was measured. The graph shows the values of the mean fluorescence intensity measured every 0.1 μm from one representative experiment out of 14–19 cells per condition.

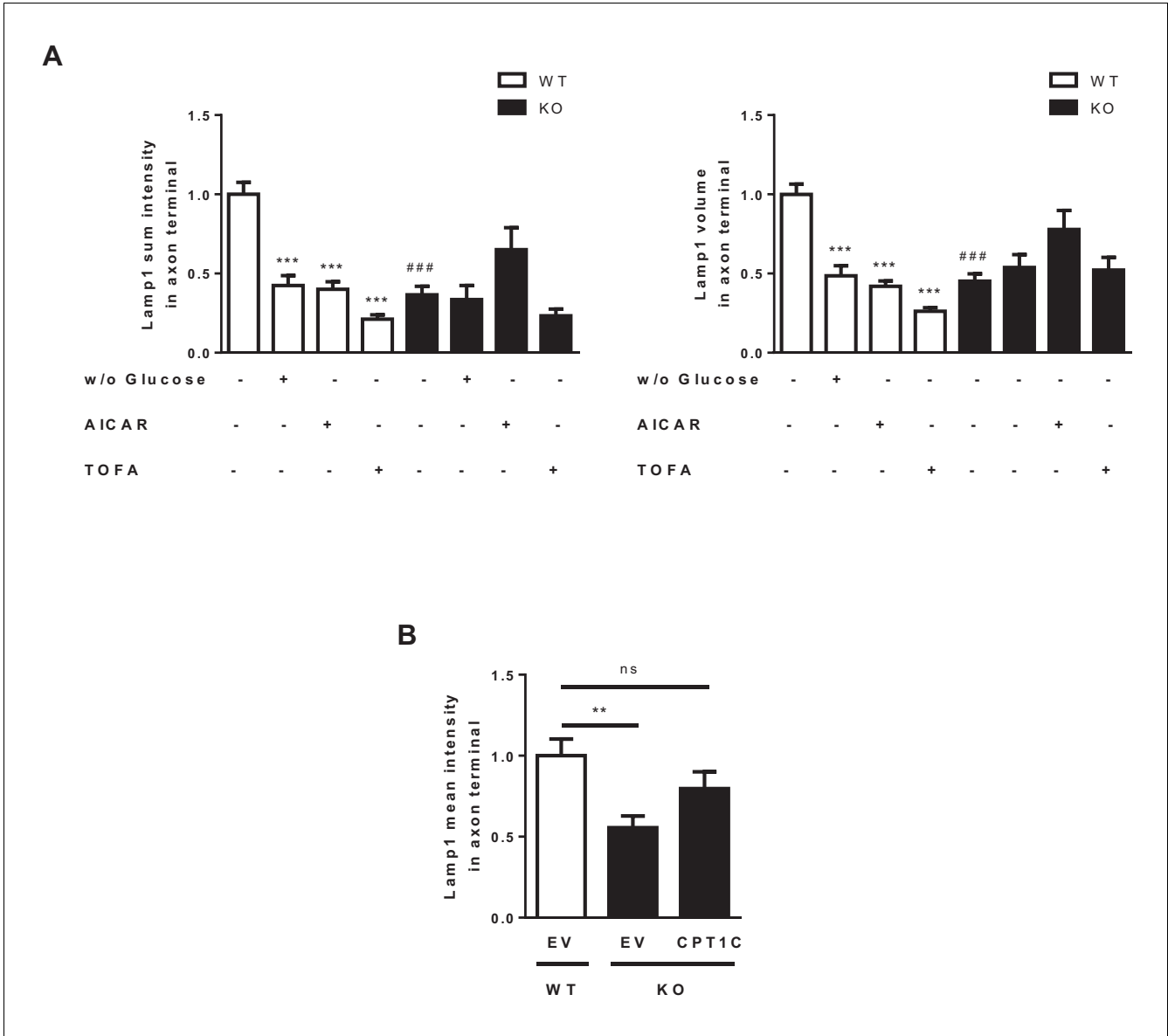


Figure 8—figure supplement 1. Metabolic stress decreases lamp1 in axon terminals through CPT1C. **(A)** Lamp1 sum intensity and the volume of Lamp1 vesicles in axon terminal were quantified. Cells were treated and processed as in **Figure 7**. Results and the mean ± SEM of 2 independent experiments performed in biological duplicates (n = 19–130 cells per condition; Two-way ANOVA followed by Bonferroni’s multiple comparison test; **p<0.01 and ***p<0.001 versus control treatment and ###p<0.01 versus WT within the same treatment). **(B)** CPT1C re-expression rescues Lamp1 intensity in axon terminals of KO neurons. Cortical neurons infected as in **Figure 1B** were stained with Lamp1. Results are the mean intensity of Lamp1 in axon terminal ± SEM of 2 independent experiments performed in biological duplicates (n = 50 cells per condition; One-way ANOVA followed by Bonferroni’s comparison test; **p<0.01 versus WT + EV).

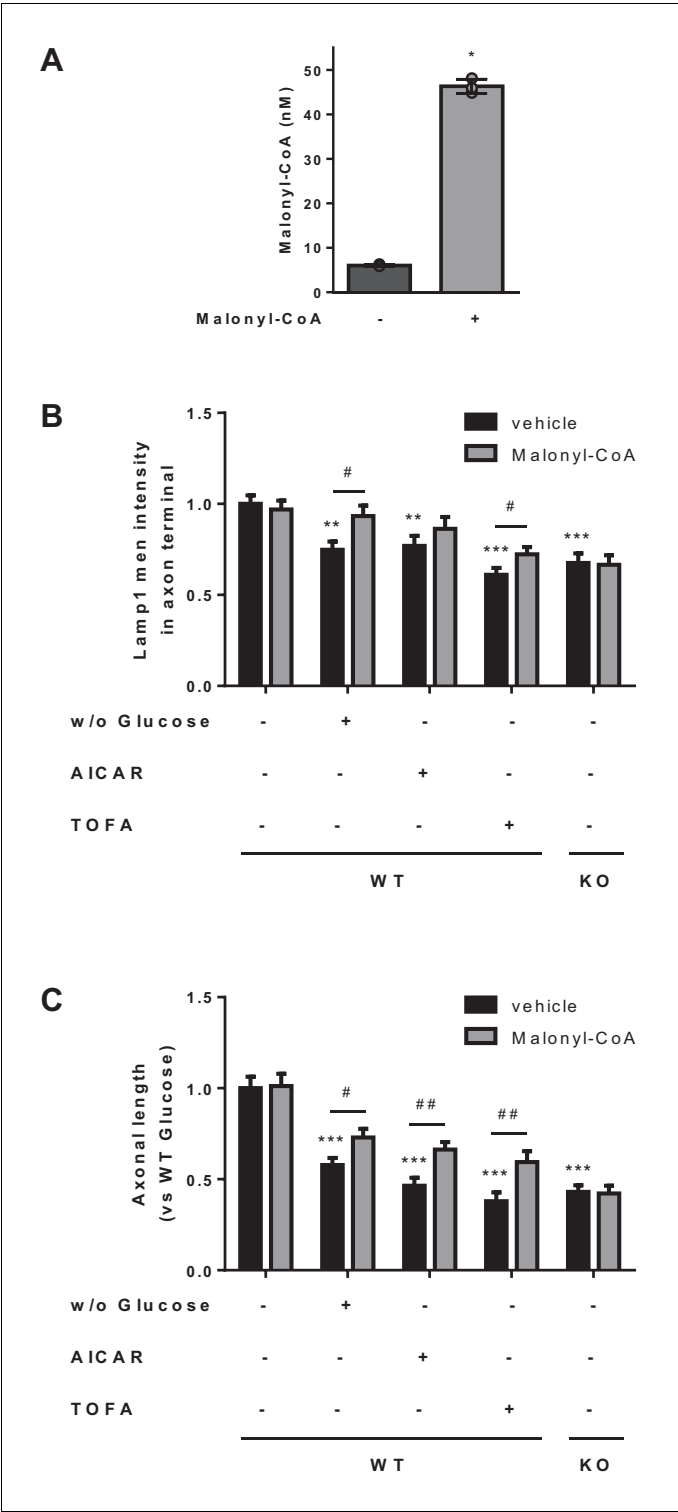


Figure 9. Malonyl-CoA partially rescues the effects of metabolic stress on axonal length and LE/Lys localization. (A) Intracellular malonyl-CoA levels. HeLa cells were treated with exogenous malonyl-CoA (200 μ M) for 2 hr and washed 3 times with PBS, collected and processed to determine intracellular levels of malonyl-CoA. Raw data are the mean of technical duplicates. Values are the mean \pm SD of triplicates ($n = 3$ samples per condition; Mann-Whitney U test; $p=0.05$). (B–C) Effect of malonyl-CoA treatment in Lamp1 intensity at the axon terminal and in axonal length. Cultured cortical neurons were treated simultaneously with malonyl-CoA (2 hr at 200 μ M) and the same conditions used in **Figure 2**. Lamp1 mean intensity at axon terminal and mean axonal length are shown in **B** *Figure 9 continued on next page*

Figure 9 continued

and C, respectively. Results are given as the mean \pm SEM of 2 independent experiment performed in biological duplicates (n = 40 cells per condition). Two-way ANOVA followed by Bonferroni's comparison test was used to compare WT in control conditions versus each treatment (*p<0.01 and ***p<0.001 versus WT in control conditions); Student's t test was applied to compare each treatment with or without malonyl-CoA (#p<0.05 versus the same condition without malonyl-CoA).

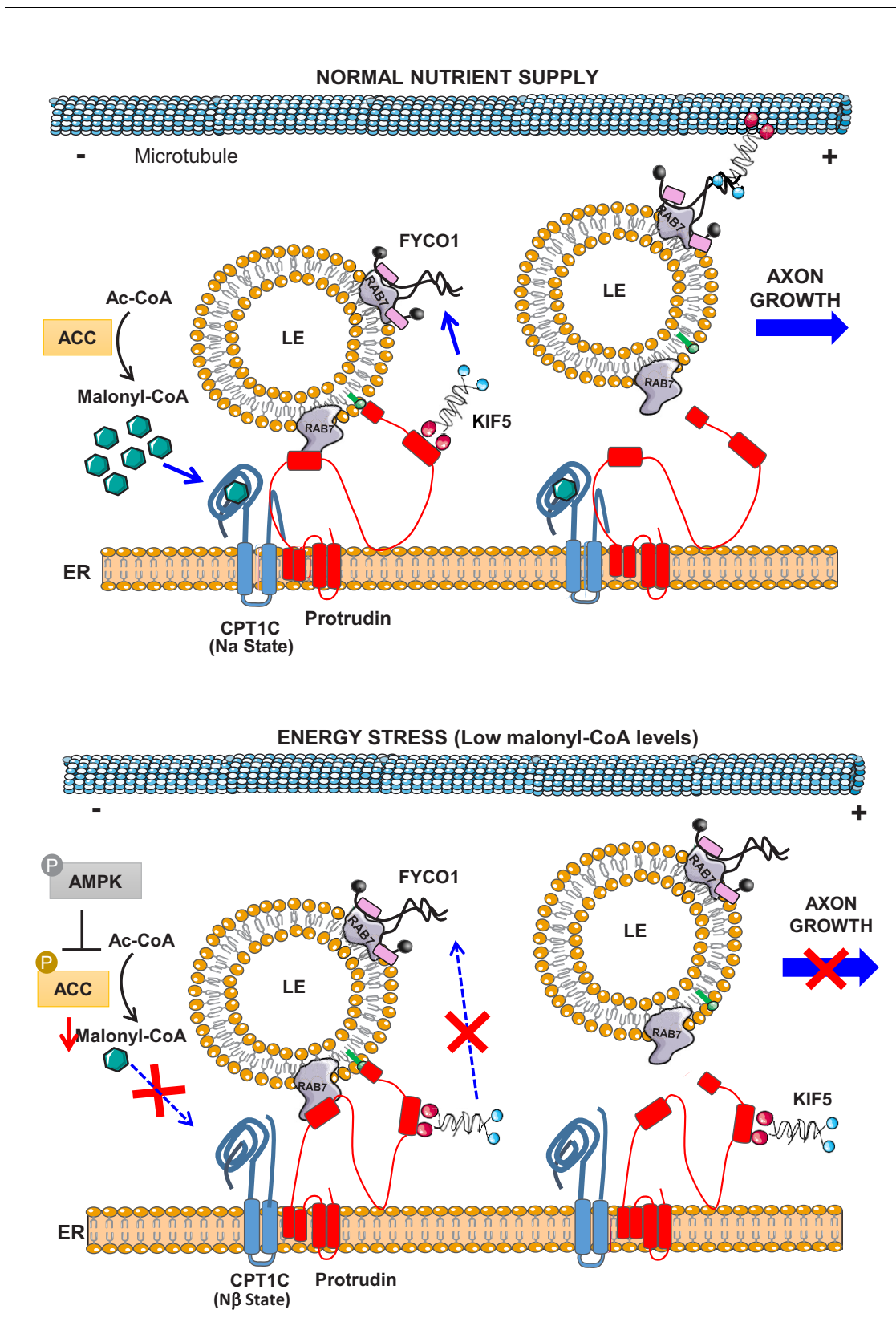


Figure 10. Model for the role of CPT1C in LE/Lys anterograde transport and axon growth. In normal nutrient conditions, CPT1C is bound to malonyl-CoA and its N-terminal domain acquires the folded conformation (N α), which enhances the transfer of kinesin-1 (KIF5) from protrudin to FYCO1, which

Figure 10 continued on next page

Figure 10 continued

promotes the plus-end transport of LE/Lys and axon growth. However, under energy stress, such as glucose depletion or the activation of AMPK pathway, N-regulatory domain of CPT1C switches to its extended conformation (N β). In this state, CPT1C does not enhance the transfer of kinesin-1 to FYCO1, and in consequence, the anterograde transport of LE/Lys is not promoted and axon growth arrested. CPT1C and protrudin are bound in both situations, but the way they interact with each other changes with metabolic stress.

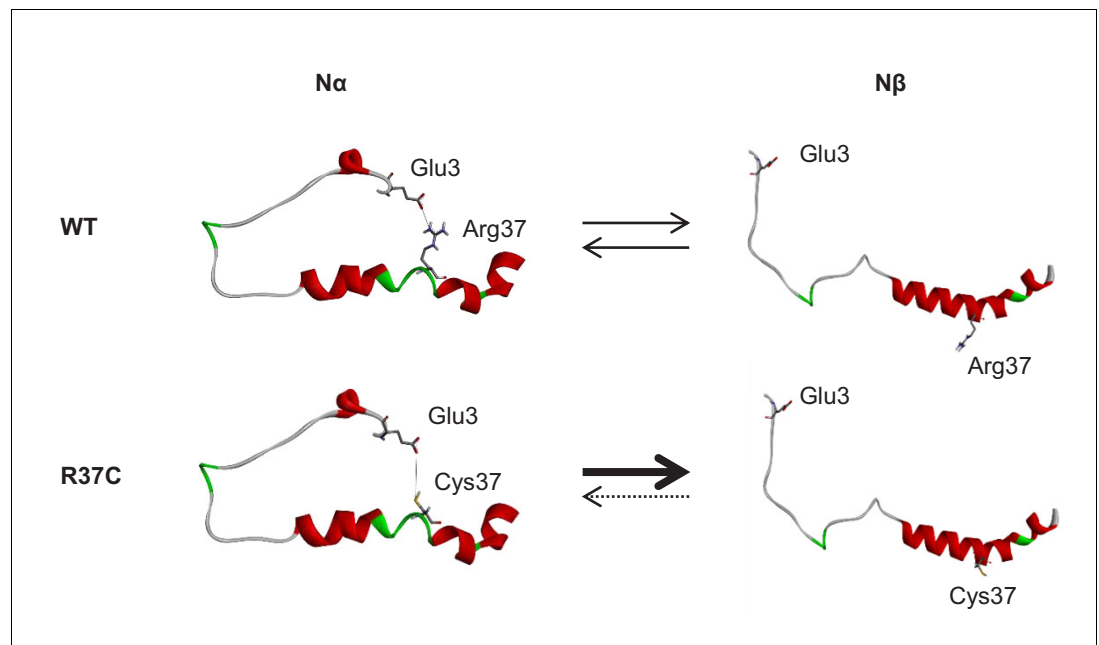


Figure 10—figure supplement 1. Effect of R37C mutation on the N-terminal domain of CPT1C. N-terminal NMR structure of CPT1C was available at PDB (accession code 2M76) (*Samanta et al., 2014*). Top: In WT sequence, there is equilibrium between N α (folded) and N β (extended) structural states. Bottom: R37C mutation causes N-terminal region of CPT1C to be preferentially in the N β state. Cys37 side chain is too short and lacks a positive charge to mimic the stabilizing electrostatic interaction observed in the WT protein.